# Ion-Exchange Kinetics: Heterogeneous Resin-Phase Model

**Abul Hasnat and Vinay A. Juvekar**
Dept. of Chemical Engineering, Indian Institute of Technology, Bombay 400076, India

*A new approach to cation-exchange kinetics views ion-exchange resin as an aggregate of uniform cylindrical pores. Ion exchange occurs at the pore surface. The counterions dissociate only partially from the fixed sites, and the charge created on the pore surface is balanced by the counterions in the electrical double layer. Thus, any cross section of a pore consists of an annular double-layer region and a central core region. Electroneutrality prevails in the core region through an influx of coions. Diffusion of ions through both regions is considered. The complete model incorporating these ideas for kinetics of monovalent cation exchange was tested with our experimental data as well as with the reported data. The pore diffusion coefficients used in the model are free ionic diffusion coefficients corrected for the tortuosity factor of the pores. Unknown parameters of the model are the degree of dissociation of counterions from the fixed sites of the pore ($f_\sigma$), and the film thickness ($\delta$). Both parameters are insensitive to the type of counterions, solution concentration, and the direction of exchange. Further, $f_\sigma$ appears to be a characteristic property of resin alone. Superiority of the developed model over the previous models is established.*

## Introduction

Understanding ion-exchange kinetics is a crucial step in the design of chromatographic separation processes using ion-exchange resins. The importance of this step is felt more strongly now in view of the recent trend towards the use of short-bed short-cycle chromatographic processes (Brown and Fletcher, 1986). It is a well-known fact that the ion exchange rate is controlled by diffusion of ions, either inside the resin particle or in the diffusion film surrounding the particle. Although, the existing models on ion-exchange kinetics correctly describe the process of diffusion in the extraparticle film (Helfferich, 1962a; Smith and Dranoff, 1964; Kraaijeveld and Wesselingh, 1993), there is sufficient ground to believe that they are not adequate in their description of intraparticle diffusion process. We illustrate this point below for the case of cation-exchange process in strong acid resins.

Strong acid cation-exchange resins are styrene-divinylbenzene polymers, with a sulfonic acid group attached to practically every phenyl ring of the polymer. The existing models, which can be called the quasi-homogeneous resin phase (QHRP) models, assume that in a swollen resin particle the sulfonic acid groups on the polymer matrix are completely solvated by the surrounding water. Moreover, since sulfonic acid is a very strong acid, it is assumed that the counterions are completely dissociated from the fixed sites and are locally uniformly distributed in the resin phase. Under this assumption, it is possible to view the resin phase as a quasi-homogeneous fluid phase in which sulfonic acid and its salts are present in the ionized state. This also allows one to assume that at any point in the resin phase, the sum of the concentrations of all the counterions equals the concentration of the fixed sites. QHRP models further assume that the partitioning of ions between the resin phase and the extraparticle fluid occurs at the outer surface of the particle which acts as the boundary between the resin and the extraparticle phases. Partitioning of the counterions is governed by the ion-exchange equilibria while that of the coions is governed by the Donnan equilibria. The above assumptions, which are due to Boyd et al. (1947), are the basis of all the existing QHRP models. The differences in various models lie only in their equations governing the diffusion process. Thus we have models based on Fick's law (Boyd et al., 1947; Reichenberg, 1953; Millar et al., 1963; Hering and Bliss, 1963; Kuo and

Correspondence concerning this article should be addressed to V. A. Juvekar.

David, 1963; Turner, 1985), Nerst-Planck equations (Helfferich and co-workers, 1957, 1958a,b, 1962a,b, 1966; Glaski and Dranoff, 1963; Smith and Dranoff, 1964; Rao and David, 1964; Morig and Rao, 1965; Turner et al., 1966; Turner and Snowdon, 1968; Bajpai et al., 1974; Weatherley and Turner, 1976; Liberti and Passino, 1985; Yoshida and Kataoka, 1985) and Stefan-Maxwell equations (Graham and Dranoff, 1982a,b; Graham, 1985; Krishna, 1987; Pinto and Graham, 1987; Kraaijeveld and Wesselingh, 1993). Here, we have attempted to critically examine the basic assumptions of the quasi-homogeneous models.

First of all, consider the assumption of complete dissociation of counterions from the fixed sites. Surface area of styrene-divinylbenzene resins ranges from 300 to 700 $m^2/g$ of dry resin (Vermeulen et al., 1984), while the resin capacity is approximately 5 meq/g of dry resin. If we assume a typical surface area of 500 $m^2/g$ and that the fixed groups are arranged on the matrix surface in the form of a square lattice, the inter-site distance can be computed to be approximately 0.4 nm. This distance is too small for the surrounding water molecules to solvate the fixed sites to any appreciable extent. Further, the surface density of the sites can be calculated to be approximately $6\times10^{18}$ sites $m^{-2}$. If we assume that the fixed sites are completely dissociated, it would develop an electric charge density of 1 $C\cdot m^{-2}$ on the matrix surface. Such a high surface charge density in conjunction with incomplete solvation of the fixed sites would give rise to very strong electrostatic repulsion among the sites. Consequently, a high electrical potential would develop on the resin matrix. Such a situation is thermodynamically untenable. It is therefore more realistic to assume that the fixed sites are only partially dissociated. From an analogy with the charge density on electrode surfaces which has the upper limit of about 0.25 $C\cdot m^{-2}$ (Bockris and Reddy, 1970), we expect the extent of dissociation of the counterions to be very small (typically less than 10%). This observation has two implications. First, it means that the total concentration of the mobile counterions, which are available for the diffusion inside the resin phase, is much smaller than $Q$, the resin capacity. Consequently, the actual diffusive fluxes of counterions are substantially lower than those predicted by QHRP models. By overestimating the intraparticle fluxes, QHRP models assign much lower resistance to intraparticle diffusion. These models, therefore, predict very high threshold values of the solution concentration, above which the intraparticle diffusional resistance becomes important. Secondly, by assigning a higher value to the driving force for the intraparticle diffusion, these models estimate lower values of intraparticle diffusion coefficients. This is evident from the fact that the self-diffusion coefficients obtained by fitting these models to the isotope-exchange data are approximately 10 to 100 times lower than the free ionic diffusion coefficients (Boyd and Soldano, 1954; Kataoka et al., 1974; Costa et al., 1984; Pinto and Graham, 1987).

Another consequence of partial dissociation of the counterions is that a high concentration of the counterions is associated with the fixed sites. These ions can indirectly participate in the diffusion process by exchanging themselves with the mobile counterions. This exchange would be governed by the local ion-exchange equilibria. The selectivity manifests itself through differences in the degree of association of different counterions with the fixed sites of the resin. Local ion-exchange equilibria can significantly modify the concentration profiles of the mobile counterions in the resin phase and thereby affect the diffusion process. From this viewpoint, exchange and diffusion of counterions become coupled processes. This viewpoint is in contrast with the QHRP models which treat the ion-exchange equilibria in the same manner as phase equilibria and hence impose them only at the phase boundary.

Yet another point of criticism that can be made against QHRP models is regarding the assumption of local uniformity of distribution of counterions. In reality, the charge on the polymer matrix results in the formation of electrical double layer. The concentration of the counterions would be highest in the vicinity of the fixed sites but would taper off in the region away from the influence of the surface charge of the fixed sites. Electroneutrality may exist in some regions where the influence of the fixed sites is absent. These regions would admit a substantial concentration of coions. This would be especially true in the case of macroporous resins where the pore radii have the dimensions of the order of 10 nm. Both the local nonuniformity of distribution of ions and the presence of coions are expected to influence the diffusion process. QHRP models, by their very nature, are unable to account for these influences.

It is evident from the above discussion that the QHRP models are inadequate to represent the various phenomena which occur inside the resin phase. High sensitivity of the estimated parameters (such as the effective diffusivity and film thickness) to the operating variables such as solution concentration, direction of exchange and the resin loading is the result of the inadequacies of these models. There is a need to develop a model which would account for the microheterogeneity in the resin phase and its effect on the diffusion process.

In this work we propose a different approach which we call the heterogeneous resin phase (RHP) model. Here we view the ion-exchange resin as an aggregate of pores. The fixed ion-exchange sites are assumed to be distributed uniformly on the walls of these pores. Only a partial dissociation of the counterions from the fixed sites of the resin is assumed. The composition of the counterions adsorbed on the fixed sites is assumed to be governed by the ion-exchange equilibria. Diffusion coefficients of the ions in the pores are free ionic diffusion coefficients corrected for the tortuosity of the pores. The tortuosity factor is calculated through the use of the Neale and Nader (1973) model. The parameters of the model are the film thickness and the degree of dissociation of counterions from the fixed sites. The cross section of a pore is divided into an annular double-layer region and a central core region. Electroneutrality is assumed to prevail in the core region, but not in the double-layer region. The total flux of a counterion in the pore is obtained by adding the fluxes in the double layer and in the core region. The concentration of the coion in the double layer is assumed to be negligibly small. For simplicity, the derivation of the model is restricted to exchange of monovalent cations. Some of the ideas presented here are based on the previous work of Bhandari et al. (1992), which is related to weak base resins.

The model has been fitted to our own experimental data and to some of the works reported in the literature. It is found

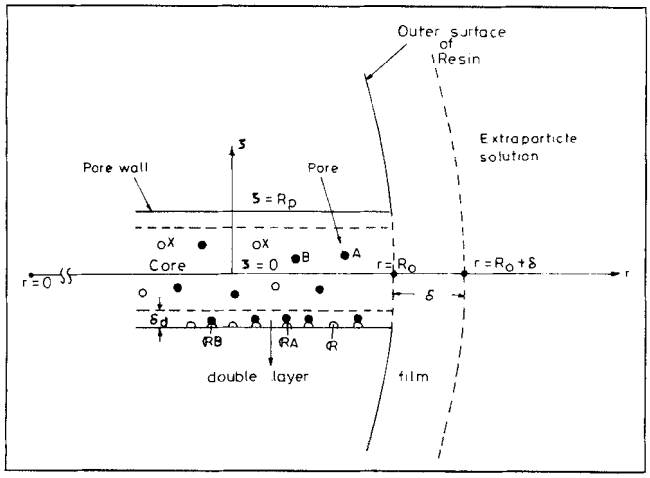


**Figure 1. Diagram of pore.**

Pores are assumed to be cylinders with uniform radius $R_p$.

that both the film thickness ($\delta$), as well as the degree of counterion dissociation ($f_\sigma$), estimated through the regression of the experimental data are insensitive to the operating variables such as resin loading, solution concentration (in the range of 1 to 200 mol·m$^{-3}$), type of counterions involved and the direction of exchange.

## Development of the Model

In our model, a cation-exchange resin particle is viewed as a sphere of radius $R_0$, consisting of a network of pores. The pores are assumed to be cylinders with uniform radius $R_p$. They are all assumed to be straight and directed radially from the center of the particle. Effect of the tortuous nature of the actual pores is lumped in tortuosity factor $\tau$, which is used for correcting the diffusivities of ions in the resin phase. Fixed ionic sites of the resin are assumed to be uniformly distributed on the walls of the pores. The fixed ionic sites is denoted by $\mathfrak{R}$ and is assumed to be monovalent. A diagram of a pore is shown in Figure 1.

Consider an exchange between two counterions $A$ and $B$, $A$ being the host ion and $B$, the invading ion. For the sake of simplicity both the counterions are assumed to be monovalent. A fixed site on the surface of the pore will be in one of the three forms $\mathfrak{R}A$, $\mathfrak{R}B$ and $\mathfrak{R}_\sigma$. The sites $\mathfrak{R}A$ and $\mathfrak{R}B$ are in association with ions $A$ and $B$ respectively. They are electrically neutral while $\mathfrak{R}_\sigma$ is the dissociated form and is negatively charged. If $Q$ is the total capacity of the resin, we can write:

$$Q = [\mathfrak{R}A] + [\mathfrak{R}B] + [\mathfrak{R}_\sigma] \tag{1}$$

where the bracketed quantities represent the concentrations of the respective species. All the concentrations, including $Q$, are expressed as moles per unit volume of the pore fluid. Composition of the pore surface ($[\mathfrak{R}A]$, $[\mathfrak{R}B]$ and $[\mathfrak{R}_\sigma]$) depends on the concentrations of $A$ and $B$ in the pore fluid. It is assumed that the pore fluid is in equilibrium with the resin surface at all times. Any nonequilibrium condition is instantly corrected by exchange of counterions between the surface and the pore fluid. The equilibrium distribution of counterions in the pore fluid varies with respect to $\zeta$ (direction perpendicular to the pore axis), due to the formation of the electrical double layer surrounding the pore surface. Any cross section of the pore in the direction perpendicular to its axis can be viewed as consisting of two regions, the annular double layer region of thickness $\delta_d$ and the central circular core region of radius $R_p$-$\delta_d$. The core region is assumed to be electrically neutral, the positive charge of the counterions being balanced by the negative charge of the coion. Here we assume that the solution contains only one type of coion $X$, which is monovalent. The concentrations of ions in the core are uniform with respect to $\zeta$ and are denoted by $[A]_c$, $[B]_c$ and $[X]_c$, respectively. Electroneutrality in the core region demands that:

$$[A]_c + [B]_c = [X]_c \tag{2}$$

The core concentrations are functions of $r$, except under the condition where the resin is in equilibrium with the extraparticle fluid in which case the core concentrations are uniform throughout the resin phase.

The electrical potential $\phi$ in the double layer may be expressed as (Morrison and Osterle, 1965):

$$\phi = \phi^c(r) + \phi^d(r, \zeta) \tag{3}$$

where $\phi^c(r)$ represents potential in the core. $\phi^d(r, \zeta)$ is the contribution to the potential due to double layer, and its value is zero in the core region.

Variation of the concentrations of the ions in the double layer can be expressed in the form of Boltzmann distribution:

$$[A]_\zeta = [A]_c \exp(-\mathfrak{F}\phi^d/RT) \tag{4}$$

$$[B]_\zeta = [B]_c \exp(-\mathfrak{F}\phi^d/RT) \tag{5}$$

$$[X]_\zeta = [X]_c \exp(+\mathfrak{F}\phi^d/RT) \tag{6}$$

The distribution of $\phi^d$ in the $\zeta$ direction can be obtained through the Poisson-Boltzmann (PB) equation:

$$\frac{1}{\zeta}\frac{d}{d\zeta}\left(\zeta\frac{d\phi^d}{d\zeta}\right) = -\frac{\mathfrak{F}}{\epsilon_r\epsilon_0}([A]_\zeta + [B]_\zeta - [X]_\zeta) \tag{7}$$

$$= -\frac{\mathfrak{F}[X]_c}{\epsilon_r\epsilon_0}[\exp(-\mathfrak{F}\phi^d/RT) - \exp(\mathfrak{F}\phi^d/RT)] \tag{8}$$

Equations 2 and 4 to 6 have been used in deriving Eq. 8 from Eq. 7.

While writing Eq. 7, we have omitted the term containing the partial derivative with respect to $r$ (distance along the axis of the pore) from the expansion of $\nabla^2\phi^d$. This is justified in view of the fact that the potential gradient in the $r$ direction is much smaller in comparison to that in the $\zeta$ direction.

Equation 8 can be solved under the following boundary conditions:

$$\text{at} \quad \zeta = R_p - \delta_d \qquad \phi^d = 0 \tag{9}$$

$$\zeta = R_p \qquad \frac{d\phi^d}{d\zeta} = -\frac{\sigma^0}{\epsilon_r\epsilon_0} \tag{10}$$

where $\sigma^0$ is the surface charge density and is related to $[\mathfrak{R}_\sigma]$ by the following equation:

$$\sigma^0 = \frac{\mathfrak{F} R_p}{2}[\mathfrak{R}_\sigma] \tag{11}$$

The double-layer thickness $\delta_d$ can be obtained by using the following boundary condition:

$$\text{at} \quad \zeta = R_p - \delta_d \qquad \frac{d\phi^d}{d\zeta} = -p \tag{12}$$

where $p$ is chosen as a small fraction of the gradient at the pore surface (that is, $\sigma^0/\epsilon_r\epsilon_0$).

In the situation where the double layer extends right up to the axis of the pore, the existence of the core region becomes fictitious. This can happen when either the pore size is very small or the total concentration of the counterions in the extraparticle solution is very low. In this case the boundary condition expressed by Eq. 9 is replaced by the following equation:

$$\text{at} \quad \zeta = 0 \qquad \frac{d\phi^d}{d\zeta} = 0 \tag{13}$$

while Eq. 12 is omitted.

## Ion-Exchange Equilibria

Consider a solution, containing counterions $A$ and $B$, in equilibrium with a cation exchange resin. The selectivity factor $\alpha$ for $B$ with respect to $A$ is defined as

$$\alpha = \frac{q_B/q_A}{[B]_0/[A]_0} \tag{14}$$

where $q_A$ and $q_B$ are the amounts of counterions $A$ and $B$ associated with the resin while $[A]_0$ and $[B]_0$ are their respective concentrations in the extraparticle solution. In computing $q_A$ and $q_B$, we may ignore the amounts of counterions in the core region since they are not strictly associated with the resin. However, we must take into account the counterions in the form of $\mathfrak{R}A$ and $\mathfrak{R}B$ and also those in the double layer region. If $q_{Ad}$ and $q_{Bd}$ are the amounts of $A$ and $B$ associated with the double layer per unit volume of the pore, charge balance in the double layer gives the following relation:

$$[\mathfrak{R}_\sigma] = q_{Ad} + q_{Bd} \tag{15}$$

Here we have ignored the charge compensation due to the coion which is present in the double layer. This is a reasonable assumption in view of a very low concentration of coions in the double layer region.

We can express $q_{Ad}$ and $q_{Bd}$ in terms of the concentrations of $A$ and $B$ in the double layer as follows:

$$q_{Ad} = \frac{[A]_c}{\pi R_p^2}\int_{R_p-\delta_d}^{R_p} \exp(-\mathfrak{F}\phi^d/RT)2\pi\zeta d\zeta \tag{16}$$

$$q_{Bd} = \frac{[B]_c}{\pi R_p^2}\int_{R_p-\delta_d}^{R_p} \exp(-\mathfrak{F}\phi^d/RT)2\pi\zeta d\zeta \tag{17}$$

where we have used Eqs. 4 and 5 to express $[A]_\zeta$ and $[B]_\zeta$ in terms of $[A]_c$ and $[B]_c$.

Taking the ratio of $q_{Ad}$ and $q_{Bd}$, we get

$$q_{Ad}/q_{Bd} = [A]_c/[B]_c \tag{18}$$

From Eqs. 15 and 18 we obtain:

$$q_{Ad} = \frac{[A]_c}{[A]_c + [B]_c}[\mathfrak{R}_\sigma] \tag{19}$$

and

$$q_{Bd} = \frac{[B]_c}{[A]_c + [B]_c}[\mathfrak{R}_\sigma] \tag{20}$$

and therefore Eq. 14 can be written as

$$\alpha = \left(\frac{[\mathfrak{R}B] + \dfrac{[B]_c}{[A]_c+[B]_c}[\mathfrak{R}_\sigma]}{[\mathfrak{R}A] + \dfrac{[A]_c}{[A]_c+[B]_c}[\mathfrak{R}_\sigma]}\right) \Bigg/ \left(\frac{[B]_c}{[A]_c}\right) \tag{21}$$

We may define equivalent fractions of $A$ and $B$ in the core as:

$$x_A^c = \frac{[A]_c}{[A]_c+[B]_c} \qquad x_B^c = \frac{[B]_c}{[A]_c+[B]_c} \tag{22}$$

and rewrite Eq. 21 as

$$\alpha = \left(\frac{[\mathfrak{R}B] + x_B^c[\mathfrak{R}_\sigma]}{[\mathfrak{R}A] + x_A^c[\mathfrak{R}_\sigma]}\right) \Big/ (x_B^c/x_A^c) \tag{23}$$

If we define equilibrium constants for adsorption of $A$ and $B$ on the fixed resin site as:

$$k_A = [\mathfrak{R}A]/x_A^c Q \qquad k_B = [\mathfrak{R}B]/x_B^c Q \tag{24}$$

Equation 23 may be rewritten as

$$\alpha = \frac{k_B + f_\sigma}{k_A + f_\sigma} \tag{25}$$

where

$$f_\sigma = [\mathfrak{R}_\sigma]/Q \tag{26}$$

$f_\sigma$, the degree of dissociation of the resin surface, represents the fraction of the fixed sites in the dissociated form.

We can consider two extreme cases of Eq. 25. For the first case we consider that all the counterions are dissociated from the pore walls. Here we have $k_A = k_B = 0$ and $f_\sigma = 1$. Equa-

tion 25 under this condition reduces to $\alpha = 1$, which means that a completely dissociated resin has no preference for either $A$ or $B$. This is obvious because all the counterions in the case of $\alpha = 1$ are associated only with the double layer which can not distinguish between $A$ and $B$. From this it can be deduced that the adsorption of counterions on the resin sites is necessary for selective ion exchange. This statement may be considered in relation to QHRP models which assume complete dissociation of the counterions from the fixed sites and yet require the resin to be selective.

The other asymptote of Eq. 25 is reached when $f_\sigma = 0$, that is, there is no dissociation of counterions from the pore surface. Equation 25 under this condition reduces to

$$\alpha^* = k_B/k_A \tag{27}$$

The ratio of $k_B/k_A$ represents the intrinsic selectivity of the resin and is denoted by $\alpha^*$. In general, the observed selectivity factor $\alpha$ lies between the two extreme limits of $\alpha^*$ and 1 depending upon the extent of dissociation of the pore surface. In practice, the value of $\alpha$, however, is expected to be nearer to $\alpha^*$ than 1 in view of a low expected value of the degree of dissociation, $f_\sigma$.

The quantities $k_A$ and $k_B$ in Eq. 24 can be considered independent of the solution composition. We cannot make such a statement regarding $f_\sigma$. The A-form of the resin may dissociate to a different extent compared to the B-form. The variation of $f_\sigma$ with solution composition would be reflected through the dependence of $\alpha$ on solution composition. In our experimental studies, we found $\alpha$ to be practically constant over a wide range of solution concentrations (1 to 200 $\text{mol}\cdot\text{m}^{-3}$) and the resin conversions. This leads us to a conclusion that the fractional dissociation of the resin pore surface $f_\sigma$ is practically independent of solution composition. We support this observation with the following argument. Since the density of the fixed ionic sites on the pore surface is very high, the total electrochemical potential of the system is dominated by the electrostatic potential of the resin surface. A very slight change in $f_\sigma$ is therefore sufficient to match the change in the chemical potential of the solution as a result of variation in its composition. At high solution concentrations, the chemical potential of the solution may become comparable to the electrical potential of the surface, in which case $f_\sigma$ may become more sensitive to the solution concentration and the resin conversion.

## Ion-Exchange Kinetics

Continuity equations for ions $A$, $B$ and $X$ in the pore fluid may be written as

$$\frac{\partial <[A]>}{\partial t} = -\frac{1}{r^2}\frac{\partial}{\partial r}(r^2 <J_A>) - \frac{\partial[\Re A]}{\partial t} \tag{28}$$

$$\frac{\partial <[B]>}{\partial t} = -\frac{1}{r^2}\frac{\partial}{\partial r}(r^2 <J_B>) - \frac{\partial[\Re B]}{\partial t} \tag{29}$$

$$\frac{\partial <[X]>}{\partial t} = -\frac{1}{r^2}\frac{\partial}{\partial r}(r^2 <J_X>) \tag{30}$$

Here we have introduced the terms $\partial[\Re A]/\partial t$ and $\partial[\Re B]/\partial t$ to account for the exchange of $A$ and $B$ with the fixed sites. This feature of our model is not present in the QHRP models.

$<[i]>$ is the area average concentration of species $i$ in the pore and $<J>$ is the area average flux. In the pores, the concentration of ion $i$ varies as a function of $\zeta$. This concentration variation results in a flux variation in the $\zeta$ direction. Averaging of the concentrations and fluxes over the area of cross section of a pore is therefore necessary. The averaging procedure is discussed in the next section. Using this procedure it is possible to express the average concentrations as well as average fluxes in terms of the core concentrations. Further, $[\Re A]$ and $[\Re B]$ can also be expressed as functions of $[A]_c$ and $[B]_c$ through Eq. 1 and Eq. 21, where both $\alpha$ and $[\Re_\sigma]$ may be considered to be constant. It is possible therefore to express all the terms of Eqs. 28–30 in terms of $[A]_c$, $[B]_c$ and $[X]_c$. Electroneutrality in the core of the pore (Eq. 2) allows us to drop one of these equations and also eliminate one of the three core concentrations. We drop Eq. 28 and eliminate $[A]_c$ from the remaining equations. The following initial and boundary conditions apply to Eqs. 29 and 30 for a batch dynamic experiment:

$$\text{at} \quad t = 0 \qquad 0 \le r \le R_0 \qquad [B]_c = 0 \qquad [X]_c = [X]_c^i \tag{31}$$

$$t > 0 \qquad r = 0 \qquad \frac{\partial[B]_c}{\partial r} = \frac{\partial[X]_c}{\partial r} = 0 \tag{32}$$

$$t > 0 \qquad r = R_0 \qquad [B]_c = [B]_s, \qquad [X]_c = [X]_s \tag{33}$$

$$\epsilon_p <J_B> = J_B^s \qquad \epsilon_p <J_X> = J_X^s \tag{34}$$

where $[X]_c^i$ is the concentration of coion in the core of the pore at the start of the experiment. For simplicity, it is assumed that $[X]_c^i$ is independent of $r$. $[B]_s$ and $[X]_s$ in Eq. 33 represent the concentrations of the respective ions in the extraparticle solution at the particle surface. $J_B^s$ and $J_X^s$ are the respective ionic fluxes in the extraparticle solution and are based on the total surface area of the resin. $\epsilon_p$ is the resin porosity and is introduced here in order to account for the difference in the area of the outer surface of the particle and the total area of the cross section of the pore mouths.

Boundary condition given by Eq. 33 implies that there is no concentration barrier for both counterion and coion at the junction of the extraparticle solution and the core of a pore (that is, at $r = R_0$). This is justifiable on the basis of the fact that the core is not under the influence of the charged resin surface and hence can establish complete continuity (in terms of chemical as well as electrical potential) with the extraparticle solution.

We adopt the film theory to account for the diffusional resistance in the solution surrounding the particle. Assuming quasi-steady state in the film, the continuity equations for the ions may be written as

$$\frac{\partial}{\partial r}(r^2 J_B) = 0 \quad \text{and} \quad \frac{\partial}{\partial r}(r^2 J_X) = 0 \tag{35}$$

Integration of the equation yields

$$J_B = \left(\frac{R_0}{r}\right)^2 J_B^s \quad \text{and} \quad J_X = \left(\frac{R_0}{r}\right)^2 J_X^s \tag{36}$$

The fluxes in the film can be expressed by Nernst-Planck (NP) equations:

$$J_i = -D_i\left[\frac{\partial[i]}{\partial r} + Z_i[i]\frac{\mathfrak{F}}{RT}\frac{\partial\psi}{\partial r}\right] \qquad i = A,\ B, \text{ and } X \tag{37}$$

where $[i]$ represents the concentration of species $i$ in the film. $D_i$ is its ionic free diffusion coefficient.

The electrical potential gradient, $\partial\psi/\partial r$, can be eliminated from Eq. 37 using no current condition:

$$\sum_i Z_i J_i = 0 \qquad Z_A = Z_B = 1 \qquad Z_X = -1 \tag{38}$$

Concentration of $A$ from the set of Eqs. 37 can be eliminated using the electroneutrality condition:

$$\sum_i Z_i[i] = 0 \tag{39}$$

The following equations for $J_B^s$ and $J_X^s$ can be derived through the above steps:

$$J_B^s = -\left(\frac{r}{R_0}\right)^2\left[\frac{D_B}{(D_B - D_A)[B] + (D_A + D_X)[X]}\right] \times\left[(D_A + D_X)[X]\frac{\partial[B]}{\partial r} - (D_A - D_X)[B]\frac{\partial[X]}{\partial r}\right] \tag{40}$$

$$J_X^s = -\left(\frac{r}{R_0}\right)^2\left[\frac{D_X}{(D_B - D_A)[B] + (D_A + D_X)[X]}\right] \times\left[(D_B - D_A)[X]\frac{\partial[B]}{\partial r} + \{2D_A[X] + (D_B - D_A)[B]\}\frac{\partial[X]}{\partial r}\right] \tag{41}$$

Equations 40 and 41 can be solved under the following boundary conditions:

$$\text{at} \quad r = R_0 + \delta; \quad [B] = [B]_0, \quad [X] = [X]_0 \tag{42}$$

$$r = R_0; \qquad [B] = [B]_s, \quad [X] = [X]_s \tag{43}$$

where $[B]_0$ and $[X]_0$ represent the bulk solution concentrations of $B$ and $X$ respectively.

The solution of the equations yield the relations between the fluxes $J_i^s$ and concentrations $[i]_s$ at particle surface.

For a batch dynamic experiment with finite solution volume, the following relations hold in the bulk of the extraparticle solution:

$$\frac{d[B]_0}{dt} = \frac{3W[B]_i}{\epsilon_p Q R_0} J_B^s \tag{44}$$

$$\frac{d[X]_0}{dt} = \frac{3W[B]_i}{\epsilon_p Q R_0} J_X^s \tag{45}$$

where $W$ is the dimensionless resin loading and is given by the following equation:

$$W = \frac{4\pi R_0^3 N \epsilon_p Q}{3[B]_i V} \tag{46}$$

Equations 44 and 45 can be solved subject to the following initial conditions:

$$\text{at} \quad t = 0 \qquad [B]_0 = [X]_0 = [B]_i \tag{47}$$

where $[B]_i$ represents the initial solution concentration of the invading ion in the extraparticle solution. The initial solution is assumed to be free from counterion A.

## Averaging of Concentrations and Fluxes in the Pore

In order to solve Eqs. 29 and 30, it is necessary to relate the area average concentrations $<[i]>$ and fluxes $<J_i>$ to the core concentrations. In this section we derive these relations.

We can express $<[i]>$ as

$$<[i]> = \frac{1}{\pi R_p^2}\left[\pi(R_p - \delta_d)^2[i]_c + \int_{R_p - \delta_d}^{R_p}[i]_\zeta 2\pi\zeta d\zeta\right] \tag{48}$$

where the first and the second terms in the bracket represent the core and the double layer contributions respectively.

For the coion we may omit the second term to the right of the above equation and can write

$$\frac{<[X]>}{[X]_c} = \left[1 - \frac{\delta_d}{R_p}\right]^2 \tag{49}$$

For counterion $B$ we can rewrite Eq. 48 using Eq. 5 as

$$\frac{<[B]>}{[B]_c} = \left[1 - \frac{\delta_d}{R_p}\right]^2 + \frac{2}{R_p^2}\int_{R_p - \delta_d}^{R_p}\exp(-\mathfrak{F}\phi^d/RT)\zeta d\zeta \tag{50}$$

To evaluate the integral on the right of Eq. 50, we make use of Eq. 8. Multiplying both the sides of Eq. 8 by $\zeta d\zeta$ and integrating between $R_p - \delta_d$ to $R_p$ we get

$$R_p\left.\frac{d\phi^d}{d\zeta}\right|_{\zeta = R_p} - (R_p - \delta_d)\left.\frac{d\phi^d}{d\zeta}\right|_{\zeta = R_p - \delta_d} = -\frac{\mathfrak{F}[X]_c}{\epsilon_r\epsilon_0}\int_{R_p - \delta_d}^{R_p}\{\exp(-\mathfrak{F}\phi^d/RT) - \exp(\mathfrak{F}\phi^d/RT)\}\zeta d\zeta \tag{51}$$

As an approximation, we drop the second term in the right-hand side of the above equation. This term represents the contribution of coion in the double layer which is negligible in most of the cases.

We also neglect the term containing $d\phi^d/d\zeta\,|_{\zeta=R_p-\delta_d}$ on the lefthand side of Eq. 51 in view of the fact that

$$\left.\frac{d\phi^d}{d\zeta}\right|_{\zeta=R_p} \gg \left.\frac{d\phi^d}{d\zeta}\right|_{\zeta=R_p-\delta_d} \tag{52}$$

These simplifications yield the following equation:

$$R_p\left.\frac{d\phi^d}{d\zeta}\right|_{\zeta=R_p} = -\frac{\mathfrak{F}[X]_c}{\epsilon_r\epsilon_0}\int_{R_p-\delta_d}^{R_p}\exp(-\mathfrak{F}\phi^d/RT)\zeta d\zeta \tag{53}$$

Using Eqs. 10 and 11 we can rewrite Eq. 53 as:

$$\int_{R_p-\delta_d}^{R_p}\exp(-\mathfrak{F}\phi^d/RT)\zeta d\zeta = \frac{R_p^2}{2}\frac{[\Re_\sigma]}{[X]_c} \tag{54}$$

In the light of Eq. 54, Eq. 50 reduces to

$$\frac{<[B]>}{[B]_c} = \left[1-\frac{\delta_d}{R_p}\right]^2 + \frac{[\Re_\sigma]}{[X]_c} \tag{55}$$

The average flux for component $i$ can be obtained through the following expression:

$$<J_i> = \frac{1}{\pi R_p^2}\left[\int_0^{R_p-\delta_d} J_i^c 2\pi\zeta d\zeta + \int_{R_p-\delta_d}^{R_p} J_i^d(\zeta)2\pi\zeta d\zeta\right] \tag{56}$$

where $J_i^c$ and $J_i^d$ denote the fluxes of component $i$ in the core and the double layer region, respectively.

In the core region, $J_i^c$ can be expressed as

$$J_i^c = -\frac{D_i}{\tau}\left[\frac{\partial[i]_c}{\partial r} + Z_i[i]_c\frac{\mathfrak{F}}{RT}\frac{\partial\phi^c}{\partial r}\right] \tag{57}$$

where $\tau$ is the tortuosity factor and $D_i$ is the free ionic diffusion coefficient for component $i$. $\tau$ is assumed to be constant at all radial locations in the particle. Both the no current condition (Eq. 38) and the electroneutrality condition (Eq. 39) are also valid in the core region. They respectively help to eliminate $\partial\phi^c/\partial r$ and $[A]_c$ from the flux expressions. The resulting equations of $J_B^c$ and $J_X^c$ are

$$J_B^c = -\frac{D_B}{\tau\{(D_A+D_X)[X]_c+(D_B-D_A)[B]_c\}} \times\left((D_A+D_X)[X]_c\frac{\partial[B]_c}{\partial r} - (D_A-D_X)[B]_c\frac{\partial[X]_c}{\partial r}\right) \tag{58}$$

$$J_X^c = -\frac{D_X}{\tau\{(D_A+D_X)[X]_c+(D_B-D_A)[B]_c\}}\left((D_B - D_A)[X]_c\frac{\partial[B]_c}{\partial r} + \{2D_A[X]_c+(D_B-D_A)[B]_c\}\frac{\partial[X]_c}{\partial r}\right) \tag{59}$$

In the double layer region, the expression for flux may be written as

$$J_i^d(\zeta) = -\frac{D_i}{\tau}\left[\frac{\partial[i](\zeta)}{\partial r} + Z_i[i](\zeta)\frac{\mathfrak{F}}{RT}\frac{\partial\phi}{\partial r}\right] \tag{60}$$

where $\phi$ is the total potential in the double layer as expressed by Eq. 3. Here we assume that the diffusivity of ion in the double layer $D_i/\tau$ is the same as that in the core region.

Expression $[i](\zeta)$ in Eq. 60 in terms of $[i]_c$ using the Boltzmann equation, we get the following general expression for the counterion flux:

$$J_i^d(\zeta) = -\frac{D_i}{\tau}\exp(-\mathfrak{F}\phi^d/RT)\left[\frac{\partial[i]_c}{\partial r} + Z_i[i]_c\frac{\mathfrak{F}}{RT}\frac{\partial\phi}{\partial r}\right] \tag{61}$$

No current condition in the double layer may be written as

$$J_A^d(\zeta) + J_B^d(\zeta) = 0 \tag{62}$$

Using the Eq. 62 we can eliminate $\partial\phi/\partial r$ from Eq. 61. The core concentration $[A]_c$ can be further eliminated from the equation for $J_B^d(\zeta)$ using the electroneutrality condition (Eq. 2). The final expression for $J_B^d$ is

$$J_B^d(\zeta) = -\frac{D_AD_B\exp(-\mathfrak{F}\phi^d/RT)}{\tau\{D_A[X]_c+(D_B-D_A)[B]_c\}}\left[[X]_c\frac{\partial[B]_c}{\partial r} - [B]_c\frac{\partial[X]_c}{\partial r}\right] \tag{63}$$

We make use of Eq. 54 to obtain

$$\int_{R_p-\delta_d}^{R_p} J_B^d(\zeta)\zeta d\zeta = -\frac{D_AD_BR_p^2[\Re_\sigma]}{2\tau[X]_c\{D_A[X]_c+(D_B-D_A)[B]_c\}} \times\left([X]_c\frac{\partial[B]_c}{\partial r} - [B]_c\frac{\partial[X]_c}{\partial r}\right) \tag{64}$$

Combining Eqs. 56 and 64 it is possible to write the area average flux of $B$ in the pore as

$$<J_B> = \left[1-\frac{\delta_d}{R_p}\right]^2 J_B^c - \frac{D_AD_B[\Re_\sigma]}{\tau[X]_c\{D_A[X]_c+(D_B-D_A)[B]_c\}} \times\left([X]_c\frac{\partial[B]_c}{\partial r} - [B]_c\frac{\partial[X]_c}{\partial r}\right) \tag{65}$$

Due to a very low concentration of the coion in the double layer region, it is expected that $J_X^d$ would be small compared to $J_X^c$ and hence it is omitted from Eq. 56. Thus, for the coion $X$, the expression for the average flux simplifies to

$$< J_X > = J_X^c \left[1 - \frac{\delta_d}{R_p}\right]^2 \tag{66}$$

Expressions 49 and 55 for the average concentrations and expressions 65 and 66 for the average fluxes in the pore can now be substituted in continuity Eqs. 29 and 30 to obtain the equations which involve only $[B]_c$ and $[X]_c$ as the dependent variables.

## Method of Solution

Equations 29 and 30 are partial differential equations involving $t$ and $r$ as the independent variables. Equations 40 and 41 are ordinary differential equations (ODEs) in $r$, while Eqs. 44 and 45 are ordinary differential equations in $t$. In this work, the orthogonal collocation technique (Villadsen and Michaelsen, 1978) was used to discretize the space derivatives along the $r$-direction in Eqs. 29 and 30. Using this technique, the partial differential equations can be converted into a set of 2N ordinary differential equations in $t$, N being the number of the internal collocation points over the interval $0 \le r \le R_0$. These ODEs along with Eqs. 44 and 45 were solved by using Harwell Library routine DC03AD which employs Gears Method. The unknown surface concentrations, $[B]_s$ and $[X]_s$ required by boundary condition 33 were obtained through the solution of Eqs. 40 and 41, using the shooting method. It was observed that 14 number of internal collocation points were sufficient to yield a solution, which was insensitive to the number of collocation points up to 4 significant figures.

For solving Eqs. 29 and 30, an initial concentration of the coion, $[X]_c^i$, is required. This value is, in general, not known. The solution was, however, found to be insensitive of $[X]_c^i$ and an arbitrary value of 10 mol·m$^{-3}$ was used throughout.

## Simplifications in the Model

Three simplifications in the above model may be considered:

(1) For microporous resins the double layer may extend up to the axis of the pore (that is, $\delta_d/R_p = 1$) especially at low solution concentrations. In this case of the core contribution to the total flux can be neglected and Eq. 65 can be reduced to

$$< J_B > = - \frac{D_A D_B [\mathfrak{R}_\sigma]}{\tau [X]_c \{D_A [X]_c + (D_B - D_A)[B]_c\}} \times \left( [X]_c \frac{\partial [B]_c}{\partial r} - [B]_c \frac{\partial [X]_c}{\partial r} \right) \tag{67}$$

while Eq. 66 can be reduced to

$$< J_X > = 0 \tag{68}$$

On the other hand in the case of macroporous resins, the pore diameter is much larger than the double layer thickness (that is, $\delta_d \ll R_p$). In this case, Eqs. 65 and 66 can be simplified by writing $\delta_d/R_p = 0$.

(2) Since the coion is not adsorbed, its holdup in the resin phase is usually very small. This allows us to assume a quasi-steady state with respect to $X$ in the pore, that is, we can drop $\partial < [X] > /\partial t$ in Eq. 30, which yields $< J_X > = 0$.

Since $< J_X >$ and $J_X^c$ are related by Eq. 66, we can write

$$J_X^c = 0 \qquad \text{at all } r \tag{69}$$

Substitution of $J_X^c = 0$ in Eq. 59 and subsequent rearrangement yields

$$\frac{d[X]_c}{d[B]_c} = - \frac{(D_B - D_A)[X]_c}{2D_A[X]_c + (D_B - D_A)[B]_c} \tag{70}$$

Equation 70 can be solved using the following boundary condition

$$[X]_c = [X]_s \qquad \text{at} \qquad [B]_c = [B]_s \tag{71}$$

Similarly, in the film we can write:

$$\frac{d[X]}{d[B]} = - \frac{(D_B - D_A)[X]}{2D_A[X] + (D_B - D_A)[B]} \tag{72}$$

with the boundary condition

$$[X] = [X]_0 \qquad \text{at} \qquad [B] = [B]_0 \tag{73}$$

Further, we can assume no change in the bulk concentration of $X$ with time. This yields

$$\text{at all} \quad t \ge 0 \qquad [X]_0 = [B]_i \tag{74}$$

Equations 70, 72, and 74 allow us to eliminate the concentrations of $X$ in Eqs. 29 and 40, thus reducing the number of equations to be solved.

(3) A further simplification occurs when $A$ and $B$ are isotopes. Here we have $\alpha = 1$ and $D_A = D_B$. Equation 21, therefore, simplifies to

$$\frac{[\mathfrak{R}A]}{[\mathfrak{R}B]} = \frac{[A]_c}{[B]_c} \tag{75}$$

In conjunction with Eq. 1, Eq. 75 yields:

$$[\mathfrak{R}A] = \frac{[A]_c (Q - [\mathfrak{R}_\sigma])}{[X]_c} \tag{76}$$

$$[\mathfrak{R}B] = \frac{[B]_c (Q - [\mathfrak{R}_\sigma])}{[X]_c} \tag{77}$$

Substitution of $D_A - D_B = 0$ in Eq. 69 gives:

$$\frac{\partial [X]_c}{\partial r} = 0 \tag{78}$$

Similarly in the film we can write

$$\frac{\partial[X]}{\partial r} = 0 \tag{79}$$

Equations 74, 78 and 79 lead us to conclude that:

$$[X] = [X]_c = [B]_i \tag{80}$$

Under these conditions Eqs. 40, 58 and 65 reduce respectively to

$$J_B^s = -D_B\left(\frac{r}{R_0}\right)^2 \frac{\partial[B]}{\partial r} \tag{81}$$

$$J_B^c = -\frac{D_B}{\tau}\frac{\partial[B]_c}{\partial r} \tag{82}$$

$$< J_B > = -\frac{D_B}{\tau}\left\{\left(1-\frac{\delta_d}{R_p}\right)^2 + \frac{[\mathfrak{R}_\sigma]}{[B]_i}\right\}\frac{\partial[B]_c}{\partial r} \tag{83}$$

With these simplifications, Eq. 29 reduces to

$$\frac{\partial[B]_c}{\partial t} = \frac{D_B}{\tau}\left(\frac{1+[\mathfrak{R}_\sigma]/[B]_i}{1+Q/[B]_i}\right)\frac{1}{r^2}\frac{\partial}{\partial r}\left(r^2\frac{\partial[B]_c}{\partial r}\right) \tag{84}$$

Equation 84 can be analytically solved under the following initial and boundary conditions:

$$t = 0 \qquad 0 \le r \le R_0 \qquad [B]_c = 0 \tag{85}$$

$$t > 0 \qquad r = 0 \qquad \frac{\partial[B]_c}{\partial r} = 0 \tag{86}$$

$$t > 0\ r = R_0 \qquad \frac{D_B}{\tau}\left(1+\frac{[\mathfrak{R}_\sigma]}{[B]_i}\right)\frac{\partial[B]_c}{\partial r}\bigg|_{r=R_0} = \frac{D_B}{\delta}([B]_0 - [B]_s) \tag{87}$$

## Validation of the Model

The model was validated using our own experimental work on batch dynamics and also some of the experimental data reported in the literature.

The unknown parameters of the model are $\tau$, the tortuosity factor, $[\mathfrak{R}_\sigma]$ the concentration of the dissociated counterions, $\delta_d/R_p$, the ratio of double layer thickness to pore radius, and $\delta$, the film thickness. The tortuosity factor was computed using the Neale and Nader (1973) model [$\tau = 2/(3 - \epsilon_p)$]. In this work, Dowex 50W X8 was used as a cation-exchange resin. This is a gel type cation-exchange resin. The average pore radius is approximately 2 nm, which is comparable to the Debye length (1 to 10 nm in the concentration range used in this study). Therefore, we expect the double layer to extend up to the pore axis. This allows us to write $\delta = R_p$ and consequently use simplified equations (Eqs. 67 and 68) for the area average fluxes. This left only two variables, viz $[\mathfrak{R}_\sigma]$ and $\delta$ to be estimated from the experimental data. Unweighted linear least square was used for regression of these parameters from experimental data. It was found that $\delta$ is very sensitive to the initial short time region of the rate data, while $\mathfrak{R}_\sigma$ is more sensitive to the latter portion. This fact considerably facilitated the procedure for the optimization of parameters.

## Experimental Studies

Fully swollen H-form resin was sieved to obtain uniform size particles with Sauter mean diameter of 0.84 mm, with standard deviation of 0.003 mm. The capacity and the water content of the resin were measured by the standard techniques described in the literature (Helfferich, 1962a) and were found to be 4.9 meq/g and 52.8% (both on dry weight basis), respectively.

The batch dynamic experiments were conducted with both the forward and the reverse exchange of H-Na and H-K pairs in the concentration range of 1–200 mol·m$^{-3}$. In all of the experiments $Cl^-$ was the coion. A glass reactor of 0.5 dm$^3$ volume with a stirrer was used. It was charged with a 0.25 dm$^3$ volume of solution. An ORION pH electrode which was connected to an E-940 ORION pH meter (with a resolution of $\pm 0.001$ pH) was dipped into the solution. The solution was first equilibrated with the electrode. A desired quantity of resin was then added and variation of the solution pH was monitored as a function of the time. All the experiments were conducted at ambient temperature ($298 \pm 1$ K) and at fixed impeller speed of 500 rpm. At this stirrer speed, resin particles were fully suspended.

## Results and Discussions

### *Fit of the model to the experimental data*

For validating the model we have used our own work (14 runs) which consists of $H^+$-$Na^+$ (H-in resin and Na-in solution), $Na^+$-$H^+$ and $H^+$-$K^+$ exchanges, the work of Tetenbaum and Gregor (1954) involves isotope exchange ($K^+$-$^{42}K^+$), work of Glaski and Dranoff (1963) involving $H^+$-$Na^+$ and $H^+$-$Cs^+$ exchanges, work of Smith and Dranoff (1965) consisting of $H^+$-$Na^+$ and $Na^+$-$H^+$ exchanges, and the recent work of Kraaijeveid and Wesselingh (1993) which involves $H^+$-$Na^+$ and $Na^+$-$H^+$ exchanges. Data are plotted as conversion of extraparticle solution, $\chi_s(t)(=[B]_0/[B]_i)$ vs. time. Some of the data are reported in terms of the conversion of the resin, $\chi_R(t)$ vs. time. $\chi_R(t)$ is calculated using the following expression:

$$\chi_R(t) = \frac{1}{4/3\pi R_0^3 Q}\int_0^{R_0}\left([\mathfrak{R}B] + [\mathfrak{R}_\sigma]\frac{[B]_c}{[X]_c}\right)4\pi r^2 dr \tag{88}$$

Free diffusivities of various ions used in this study are calculated from ionic mobilities (Robinson and Stokes, 1959). The calculated values are $D_H$, $9.31\times10^{-9}$ m$^2$·s$^{-1}$; $D_{Na}$, $1.33\times10^{-9}$ m$^2$·s$^{-1}$; $D_K$, $1.95\times10^{-9}$ m$^2$·s$^{-1}$; $D_{Cs}$, $2.05\times10^{-9}$ m$^2$·s$^{-1}$; $D_{Cl}$, $2.03\times10^{-9}$ m$^2$·s$^{-1}$; $D_{NO_3}$, $1.90\times10^{-9}$ m$^2$·s$^{-1}$. The following values of selectivities were experimentally obtained. For $\alpha_{H^+-Na^+} = 1.53$ and $\alpha_{K^+-H^+} = 2.20$. The selectivity, $\alpha_{Cs^+-H^+}$, was taken to be 2.54 (Anderson, 1988).

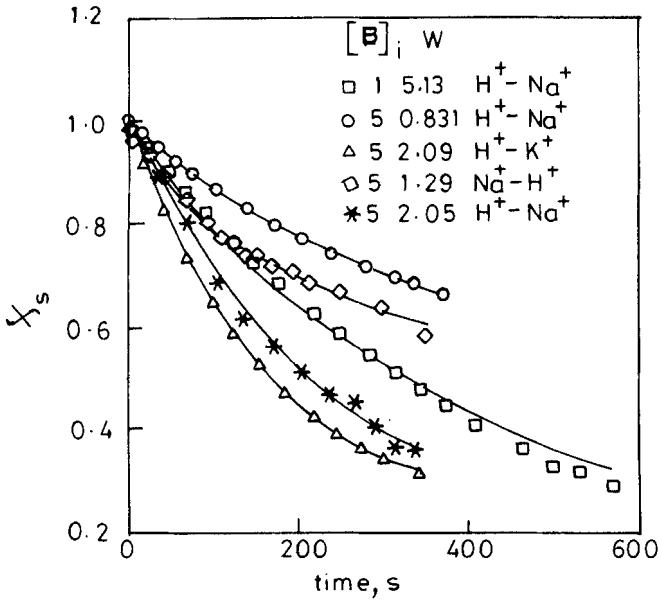


**Figure 2. Typical fits of the model to experimental data.**

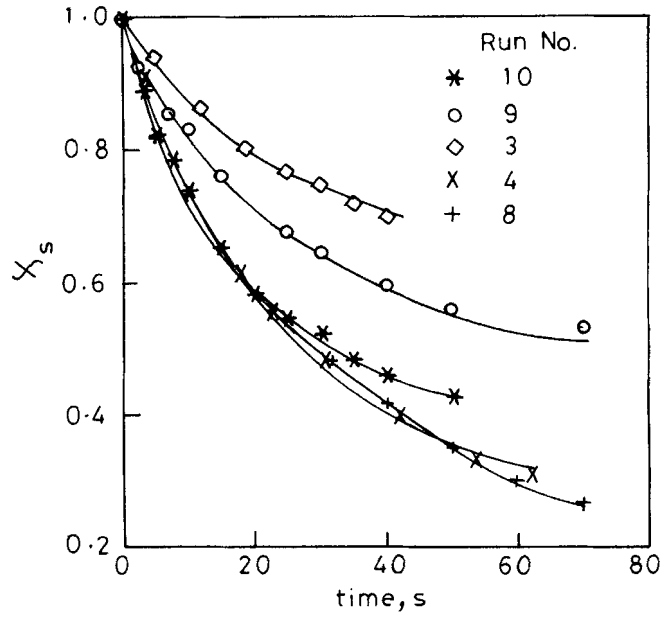


**Figure 4. Typical fits of the model to experimental data.**

A few typical fits of the model to our experimental data are shown in Figures 2 and 3 while those of others are shown in Figures 4 to 6. It is seen from these figures that the model fits the experimental data in excellent manner in most cases.

### *Comments on the regression estimates of $\delta$ and $f_\sigma$*

The regression estimates of $\delta$ and $f_\sigma$ from our work have been listed in Table 1, while those from the other works have been listed in Table 2. Values of standard deviations of the experimental data from the model fit are also listed in the tables.

Since in our experimental work we have used a constant stirrer speed, the value of $\delta$ is expected to be the same in all the experiments. Table 1 confirms this. The average value of $\delta$ from Table 1 is 3.23 $\mu$m with a maximum deviation of 10%. Data from the Table 2 also indicate that except for the work of Tetenbaum and Gregor (1954), value of $\delta$ is practically same for all the data points of a given work. This again is expected in view of the constant speed of agitation used in these works. The data of Tetenbaum and Gregor (1954) are in a fixed bed with varying fluid velocity $\delta$ here is seen to decrease with increase in the superficial liquid velocity, which also is in concurrence with the expectation.

The regression values of $f_\sigma$ obtained from our work are nearly constant over the entire range of solution concentrations (1 to 200 mol·m$^{-3}$). The average value of $f_\sigma$ is 0.0408

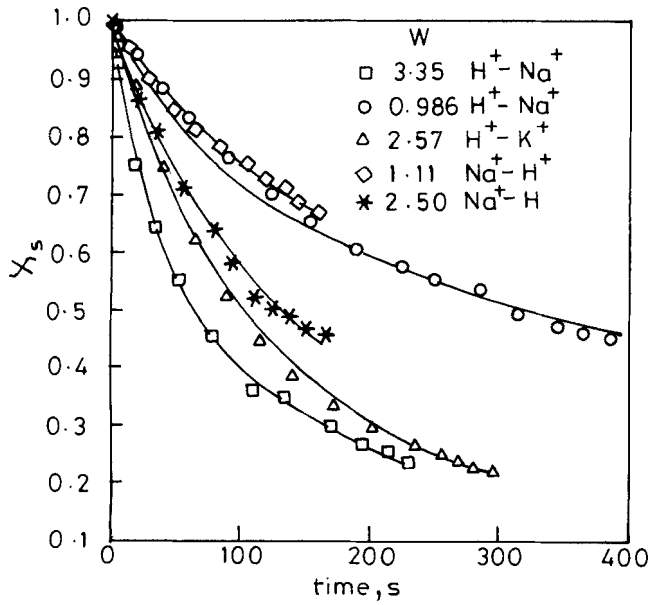


**Figure 3. Typical fits of the model to experimental data.**

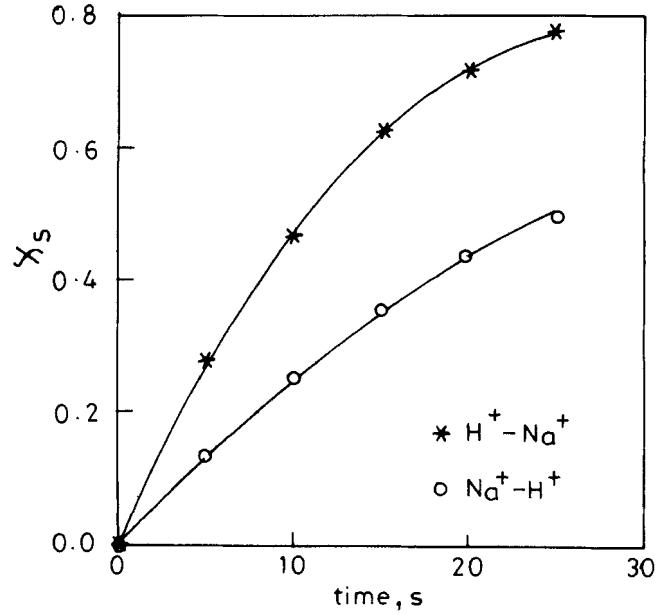


**Figure 5. Typical fits of the model to experimental data.**

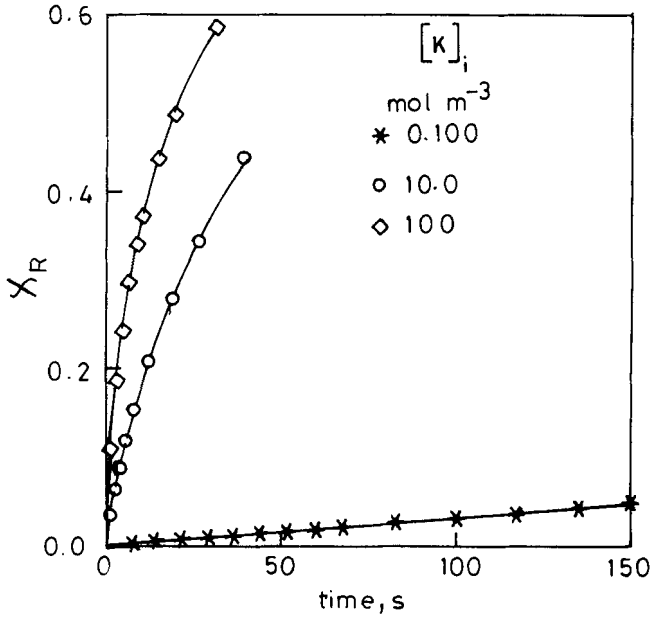


**Figure 6. Typical fits of the model to experimental data.**

with a standard deviation 6.7%. It is also seen that $f_\sigma$ is independent of the type of the ions participating in the exchange process, resin loading and the direction of exchange. However, $f_\sigma$ appears to depend upon the type of the resin used as seen by comparing the value of $f_\sigma$ obtained from the data of Tetenbaum and Gregor with that obtained from other cases (12% cross-linking in the resin used by Tetenbaum and Gregor, 8% in other cases).

### *Relative importance of the film resistance to diffusion*

The simulated plot of dimensionless surface concentrations of invading ion $B_s$ vs. resin conversion (Figure 7) can be used to illustrate the relative importance of film resistance and pore resistance in ion-exchange process. The extraparticle solution concentration is used as the parameter. The simulation is done with $\alpha = 1.53$, $f_\sigma = 0.04$ and $\delta = 3$ $\mu$m.

Small value of $B_s$ ($B_s \ll 1$) is indicative of dominance of film diffusion. The dominance of the pore diffusion is indicated when $B_s$ approaches one. Both the resistances are important for the intermediate cases. The plot clearly shows that even at low solution concentration (1 mol·$m^{-3}$) film resistance is not dominant over the entire range of resin conversions. With increase in conversion, the pore diffusion resistance becomes increasingly important. It is therefore impossible, except at very low solution concentration and very high resin loading, to have a situation in which film controlled

**Table 1. Regression Estimates of HRP Model Parameters Using Our Experimental Data***

| Host Ion | Invading Ion | Initial Solution Conc. mol·$m^{-3}$ | Resin Loading W | $\delta$ $\mu$m | $f_\sigma$ $\times 10^2$ | $\sigma_d^\dagger$ $\times 10^3$ |
|---|---|---|---|---|---|---|
| H | Na | 1.00 | 5.13 | 3.11 | 4.25 | 1.33 |
| H | Na | 5.00 | 2.05 | 3.81 | 4.07 | 2.67 |
| H | Na | 5.00 | 0.831 | 3.50 | 3.99 | 6.88 |
| H | K | 5.00 | 2.10 | 3.19 | 4.10 | 3.16 |
| Na | H | 5.00 | 1.28 | 3.07 | 4.17 | 4.91 |
| H | Na | 10.0 | 3.35 | 3.01 | 3.89 | 4.20 |
| H | Na | 10.0 | 0.986 | 3.12 | 3.87 | 5.21 |
| H | K | 10.0 | 2.58 | 3.41 | 4.04 | 1.02 |
| Na | H | 10.0 | 2.50 | 3.13 | 4.38 | 3.21 |
| Na | H | 10.0 | 1.11 | 3.28 | 4.07 | 3.55 |
| H | Na | 100 | 0.984 | 2.86 | 3.82 | 2.41 |
| H | K | 100 | 1.23 | 3.12 | 3.87 | 4.72 |
| Na | H | 100 | 0.735 | 3.60 | 4.28 | 2.11 |
| H | Na | 200 | 0.984 | 3.07 | 4.42 | 4.68 |

*Resin: Dowex 50W $X8$.

$^\dagger\sigma_d = \left[\frac{1}{n-1}\sum_{i=1}^{n}\left(\chi_s^{\text{expt}}(i) - \chi_s^{\text{model}}(i)\right)^2\right]^{1/2}$

where $n$ is the number of observations.

**Table 2. Regression Estimates of HRP Model Parameters Using Published Data**

| Host Ion | Invading Ion | Initial Solution Conc. mol·$m^{-3}$ | Resin Loading (W) | Impeller Speed RPM Superf. Liq. Vel. m·$s^{-1}$ | $\delta$ $m \times 10^6$ | $f_\sigma$ $\times 10^2$ | $\sigma_d$ $\times 10^3$ |
|---|---|---|---|---|---|---|---|
| *Glaski and Dranoff (1963), Dowex 50W X8* | | | | | | | |
| H | Na | 10.0 | 1.00 | Not | 70.0 | 3.98 | 5.62 |
| H | Cs | 9.60 | 2.00 | reported | 63.0 | 4.02 | 1.01 |
| *Smith and Dranoff (1965), Dowex 50W X8* | | | | | | | |
| H | Na | 10.0 | 2.37 | 1,750 | 23.0 | 3.47 | 2.44 |
| Na | H | 10.0 | 2.32 | | 23.1 | 3.46 | 3.05 |
| Na | H | 10.0 | 1.56 | | 20.8 | 3.25 | 1.99 |
| *Kraaijeveld and Wesselingh (1993), Lewatit S100* | | | | | | | |
| H | Na | 10.0 | 23.8 | 900 | 9.50 | 4.01 | 6.56 |
| Na | H | 10.0 | 23.8 | | 8.51 | 4.50 | 5.56 |
| *Tetenbaum and Gregor (1954), Polystyrenesulfonic (12% Cross-linked)* | | | | | | | |
| $^{42}$K | K | 100 | * | | 3.46 | 0.510 | 6.81 | 2.01 |
| $^{42}$K | K | 0.10 | * | | 2.53 | 0.585 | 9.13 | 4.71 |
| $^{42}$K | K | 10.0 | * | | 2.30 | 0.710 | 7.78 | 3.93 |

*Exchange is carried out in fixed bed.

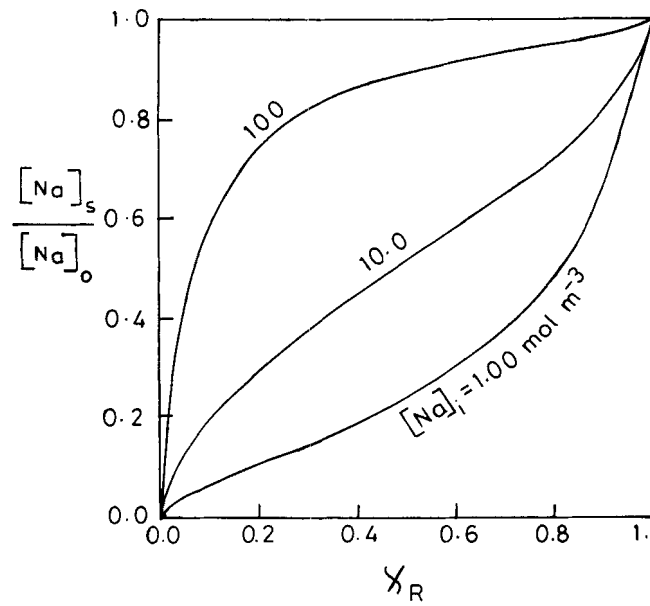


**Figure 7. Simulated plot of dimensionless surface concentrations of invading ion $B_s$ vs. resin conversion.**

regime prevails over the entire range of the resin conversion. It is also seen from Figure 7 that at low solution concentrations, there is a gradual increase in the surface concentration with time. On the other hand, at high solution concentrations the surface concentration increases sharply with time. This variation can be explained as follows. The film diffusion flux increases in proportion to solution concentration. As a result, the film diffusion resistance decreases with increase in the solution concentration while the pore diffusion resistance remains approximately constant. The film diffusion resistance therefore dominates over a wider range of the resin conversions at the low solution concentrations than at the high solution concentrations.

### *Donnan exclusion*

To estimate the extent of Donnan exclusion predicted by HRP model, we have simulated the Poisson-Boltzmann equation in cylindrical coordinates with three different pore diameters. The value of $f_\sigma$ of 0.04 is used. From $f_\sigma$, the surface charge density is calculated through Eq. 11. The concentration, $<[X]>$ of the coion in pores is calculated by averaging $[X]_\xi$ over the area of cross section of the pore.

Table 3 lists the values of $<[X]>$ and the extent of exclusions of the coion from the pores for some solution concentrations. It is clear from the table that the average concentration of the coion in the resin phase increases almost linearly with the increase in solution concentrations as observed by Boyd and Bunzl (1967). Although our model predicts substantial exclusion of coion in the range of solution concentration of 1 and 10 mol·m$^{-3}$, the extent of exclusion is substantially lower than that predicted by the ideal Donnan equilibrium.

### *Relative magnitude of double layer and core fluxes*

The contribution of the flux through the core region of the pores would be important in the case of macroporous resins where the core would span the major portion of the area of cross section of pore. It is therefore worthwhile to determine the relative magnitude of the core and the double layer fluxes.

Figure 8 is a simulated plot showing variation of $J_B^d|_{r=R_0}$ and $J_B^c|_{r=R_0}$ with the resin conversion. The simulation is done for $H^+$-$Na^+$ exchange with $\alpha = 1.53$, $f_\sigma = 0.04$. The particle surface concentration $B_s$ is used as the parameter. It is clear

**Table 3. Extent of Donnan Exclusion by HRP Model***

| Pore Dia. nm | Solution Conc., $[X]$ mol·m$^{-3}$ | Area Avg. Conc. in Pore, $<[\bar{X}]>$ mol·m$^{-3}$ | Deg. of Excl. $(1 - <[X]>/[X]) \times 10^2$ |
|---|---|---|---|
| 0.8 | 1.00 | $2.12\times10^{-3}$ | 99.7 |
| | 10.0 | $2.13\times10^{-2}$ | 97.8 |
| | 100 | 0.217 | 78.3 |
| 1 | 1.00 | $3.32\times10^{-3}$ | 99.6 |
| | 10.0 | $3.35\times10^{-2}$ | 96.6 |
| | 100 | 0.324 | 67.5 |
| 2 | 1.00 | $1.32\times10^{-2}$ | 98.2 |
| | 10.0 | 0.132 | 86.8 |
| | 100 | 0.697 | 30.3 |

*Resin: Dowex 50W X8, $f_\sigma = 0.04$.

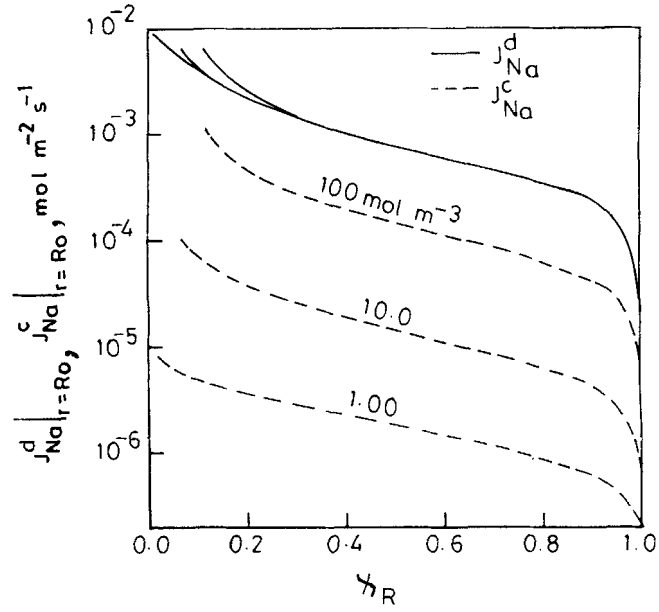


**Figure 8. Simulated plot showing variation of $J_B^d|_{r=Ro}$ and $J_B^c|_{r=Ro}$ with the resin conversion.**

from this plot that $J_B^d$ is independent of the solution concentration. This is expected since the double layer flux is caused by dissociation of counterions from the internal resin surface and the extent of this dissociation is independent of the solution concentration. On the other hand, $J_B^c$ varies almost linearly with the solution concentration as seen from the plot. As a consequence, the relative magnitude of $J_B^c$ to the total flux increases with the increase in solution concentration. Thus at a solution concentrations of 1 and 10 mol·m$^{-3}$, the core flux is negligible compared to the double layer flux and the total flux is entirely made of the double layer flux. At about the concentration of 100 mol·m$^{-3}$, the magnitude of core flux becomes significant in comparison to double layer flux. This leads us to conclude that the contribution of the core flux to the total flux cannot be neglected for the concentration above 100 mol·m$^{-3}$.

## Comparison with a quasi-homogeneous resin phase model

A QHRP model was used to fit our experimental data. The model equations were written under the following assumptions:

(1) The diffusion fluxes of the ions both in the resin and extraparticle phases were represented by the Nernst-Planck equations.

(2) Equilibrium was assumed to exist at the particle-fluid interface.

(3) The film was assumed to be flat. The quasi-steady state was assumed in describing the diffusion process in the film.

(4) The coion was completely excluded from the resin phase. The flux of coion in the extraparticle fluid was assumed to be zero.

A combined model incorporating the effects of both the film and the particle diffusion resistances was used. The model had three parameters, namely, diffusion coefficients

Table 4. Regression Estimates of QHRP Model Parameters*

| Host Ion | Invad. Ion | Init. Sol. Concentration $mol \cdot m^{-3}$ | Resin Loading W | $\delta$ $\mu m$ | $\bar{D}_A$ $m^2 \cdot s^{-1}$ $\times 10^9$ | $D_A/\bar{D}_A$ | $\bar{D}_B$ $m^2 \cdot s^{-1}$ $\times 10^9$ | $D_B/\bar{D}_B$ | $\sigma_d$ $10^3$ |
|---|---|---|---|---|---|---|---|---|---|
| H | Na | 1.00 | 5.13 | 5.66 | | | | | 3.71 |
| H | Na | 5.00 | 2.05 | 6.76 | | | | | 2.92 |
| H | Na | 5.00 | 0.831 | 8.52 | | | | | 6.10 |
| H | K | 5.00 | 2.10 | 6.08 | | | | | 3.35 |
| Na | H | 5.00 | 1.28 | 7.01 | | | | | 9.54 |
| H | Na | 10.0 | 3.35 | 11.5 | | | | | 2.74 |
| H | Na | 10.0 | 0.986 | 12.5 | | | | | 4.19 |
| H | K | 10.0 | 2.58 | 9.50 | | | | | 5.39 |
| Na | H | 10.0 | 2.50 | 14.1 | | | | | 7.26 |
| Na | H | 10.0 | 1.11 | 13.2 | | | | | 3.15 |
| H | Na | 100 | 0.984 | 12.8 | 1.22 | 7.60 | 0.0955 | 13.9 | 7.20 |
| H | K | 100 | 1.23 | 9.81 | 2.56 | 3.63 | 0.152 | 13.0 | 3.11 |
| Na | H | 100 | 0.735 | 15.3 | 0.362 | 3.67 | 2.95 | 3.15 | 8.01 |
| H | Na | 200 | 0.984 | 12.9 | 1.07 | 8.70 | 0.0910 | 14.6 | 5.72 |

*Resin: Dowex 50W×8.

($\bar{D}_A$ and $\bar{D}_B$) in the resin phase and the film thickness ($\delta$). The model was fitted to the experimental data obtained in the present work. The unweighted least-square technique was used for the optimization of the parameters. Optimization was carried out using VA05AD subroutine of Harwell library. Results of the simulation are reported in Table 4.

For the dilute solutions (1 to 10 $mol \cdot m^{-3}$), the experimental data was insensitive to the values of effective diffusivities. Hence, in this range of concentrations, only the values of $\delta$ are reported in Table 4. In the higher range of solution concentrations (100 and 200 $mol \cdot m^{-3}$), it was possible to estimate all the three parameters. Table 4 also lists the retardation factors, $D_A/\bar{D}_A$ and $D_B/\bar{D}_B$, where $D_i$ is the free diffusion coefficient of ion $i$.

It is seen from this table that the estimated values of the film thickness (5–14 $\mu m$) are substantially higher than that obtained through the use of HRP model (an average value of 3.23 $\mu m$). Moreover, $\delta$ is not constant, but increases with increase in the solution concentration, while for a fixed solution concentration it increases with decrease in the resin loading. These observations can be easily explained on the basis of our model. As pointed out earlier, the QHRP models lump a large part of the intraparticle diffusion resistance with the film diffusion resistance. For the solution concentrations less than 100 $mol \cdot m^{-3}$, the entire intraparticle diffusional resistance is lumped in $\delta$. Hence, the estimated values of $\delta$ are higher than the actual. With a decrease in the resin loading, the intraparticle diffusional resistance increases relative to the film diffusion resistance because lower resin loading implies higher resin conversion and hence longer intraparticle diffusional path length. Similarly, with increase in the solution concentration, the film-flux increases relative to the intraparticle-flux, the latter being independent of the solution concentration. Both these changes result in higher values of $\delta$. It is also seen that under otherwise the same conditions, $\delta$ is lower with potassium than with sodium. This is due to the fact that potassium ion diffuses faster inside the resin and hence has a lower intraparticle diffusional resistance which is reflected in lower value of $\delta$.

Inspection of the resin phase coefficients ($\bar{D}_A$ and $\bar{D}_B$) reveals that the slower moving ions ($K^+$ and $Na^+$) show the retardation factor of 13 to 14 when they are in the extraparticle solution and the factor of 3 to 4 when they are in the resin phase. On the other hand, $H^+$ when paired with $Na^+$ ion exhibits the retardation factor of 7 to 8 when it is inside and a factor of 3 when outside. Retardation factor also seems to depend on the pairing ions. Retardation with $K^+$ as pairing ion is about half of that with $Na^+$ as pairing ion. Such a wide variation in retardation factors makes the applicability of the model questionable at least in the range of solution concentrations used in our experiment.

### *Range of applicability of HRP model*

(1) In the development of the model, we have considered a resin with unimodal pore structure. The model is applicable to, say, biporous resin only if the diffusional resistance in the micropores is small enough to permit us to assume that all the resin capacity is concentrated on the surface of the macropores. However, we would like to point out that this assumption is unlikely to be violated in most cases. This is because the micropores are situated in the walls of the macropores where the concentration of a counterion is much higher than the core concentration. The diffusional driving force in the micropores is therefore expected to be much higher than in the macropores. This, coupled with shorter lengths of micropores, would make the micropore resistance unimportant in most cases.

(2) The model is expected to be directly applicable to the normal ion exchange in weak acid resins (Type II process of Helfferich, 1965 classification). Weak acid resins are expected to differ from the strong acid resins only in the degree of dissociation for counterions from the fixed sites.

(3) The model is also applicable to the kinetics of anion exchange in strong base resins provided the size of the anions are substantially lower than the pores.

(4) The HRP model can be extended to study the diffusion of ion-exchange membranes. The equations, however, need modifications to take into account the convective transfers of solvent and ions.

(5) Although the model developed here can, in principle, be extended to ion exchange involving multivalent cations, a number of difficulties arise in the process of extension. First, the averaging technique for flux and concentration becomes more complicated when the cation participating in the exchange has different valences and needs the solution of the Poisson-Boltzmann equation. Further, we feel that unlike the monovalent ions the extent of dissociation $f_\sigma$ of a resin may depend upon the surface composition. A more detailed study is needed in order to extend the model for multivalent cases. An effort towards this is currently underway in this laboratory.

## Conclusion

The HRP model presented in this article provides a deeper insight into the kinetics of ion exchange. Using this model, it has been possible to clearly segregate the intraparticle and the extraparticle diffusional resistances. The model has also been able to quantify the effects of local ion-exchange equilibria, electrical double layer formation, and the adsorption of counterions on the fixed sites on the kinetics of ion exchange.

## Notation

$[A]$ = concentration of $A$, mol·m$^{-3}$
$[B]$ = concentration of $B$, mol·m$^{-3}$
$[B]_i$ = initial concentration of B in the solution, mol·m$^{-3}$
$B_s$ = dimensionless particle surface concentration of counterion, $B$
$D$ = free diffusion coefficient of ion, m$^2$·s$^{-1}$
$f_\sigma$ = extent of dissociation of counterions from fixed sites, dimensionless
$\mathfrak{F}$ = Faraday constant, C·mol$^{-1}$
$J$ = diffusional flux of ion, mol·m$^{-2}$·s$^{-1}$
$k_A, k_B$ = adsorption constants for counterions $A$ and $B$
$q_A, q_B$ = total amounts of counterions ($A$ and $B$ respectively) associated with the pore surface, mol·m$^{-3}$ of pore volume
$q_{Ad}, q_{Bd}$ = amounts of counterions ($A$ and $B$ respectively) associated with the double layer, mol·m$^{-3}$ of pore volume
$Q$ = capacity of the resin based on pore volume, mol·m$^{-3}$
$r$ = radial location in the resin particle, m
$R$ = universal gas constant, J·K$^{-1}$mol$^{-1}$
$R_o$ = radius of resin particle, m
$R_p$ = radius of pore, m
$\mathfrak{R}A$, $\mathfrak{R}B$ = ion pair of $A$ and $B$ respectively with fixed site, $\mathfrak{R}$, of resin
$\mathfrak{R}_\sigma$ = free (dissociated) ionic site of resin
$t$ = time, s
$T$ = temperature, K
$N$ = total number of resin particles in system
$V$ = volume of solution, m$^3$
$x$ = ionic fraction defined in Eq. 22
$[X]$ = coion concentration, mol·m$^{-3}$

### *Greek letters*

$\delta$ = film thickness, m
$\delta_d$ = double layer thickness, m
$\epsilon_0$ = absolute permittivity of the medium, J$^{-1}$·C$^2$·m$^{-1}$
$\epsilon_p$ = fractional pore volume, dimensionless
$\epsilon_r$ = relative permittivity of the medium, dimensionless
$\zeta$ = distance measured in the direction normal to the pore axis, m
$\sigma^0$ = surface charge, C·m$^{-2}$
$\phi$ = contribution to electrical potential due to double layer, V
$\phi^c$ = electrical potential in the core, V
$\chi_s(t)$ = solution conversion, dimensionless
$\chi_R(t)$ = resin conversion, dimensionless
$\psi$ = total electrical potential, V

### *Subscripts*

$i$ = initial state and ionic species
0 = bulk solution
$s$ = particle surface

### *Superscripts*

$c$ = core
$d$ = double layer
$-$ = resin phase

## Literature Cited


Anderson, R. E., "Ion-Exchange Separations," *Handbook of Separation Techniques for Chemical Engineers*, 2nd ed., P. A. Schweitzer, ed., McGraw-Hill, New York (1988).

Bajpai, R. K., A. K. Gupta, and M. Gopala Rao, "Single Particle Studies of Binary and Ternary Ion Exchange Kinetics," *AIChE J.*, **20**(5), 989 (1974).

Bhandari, V. M., V. A. Juvekar, and S. R. Patwardhan, "Sorption Studies on Ion Exchange Resin. 1. Sorption of Strong Acids in Weak Base Resins," *Ind. Eng. Chem. Res.*, **31**, 1060 (1992).

Bockris, J. O. M., and A. K. N. Reddy, *Modern Electrochemistry*, Vol. 2, Plenum Press, New York, p. 747 (1970).

Boyd, G. E., and K. Bunzl, "The Donnan Equilibrium in Cross-Linked Polystyrene Cation and Anion Exchangers," *J. Amer. Chem. Soc.*, **89**(8), 1776 (1967).

Boyd, G. E., and B. A. Soldano, "Self-Diffusion of Cations in and Through Sulphonated Polystyrene Cation Exchange Polymers," *J. Amer. Chem. Soc.*, **75**(24), 6091 (1954).

Boyd, G. E., A. W. Adamson, and L. S. Myers, Jr., "The Exchange Adsorption of Ions from Aqueous Solutions by Organic Zeolites: II. Kinetics," *J. Amer. Chem. Soc.*, **60**, 836 (1947).

Brown, C. J., and C. J. Fletcher, "Water Deionization by Recoflo Short Bed Ion Exchange," *Proc. Int. Water Conf.*, Pittsburgh (Oct. 27–29, 1986).

Costa, E., A. de Lucas, and M. E. Gonzalez, "Ion Exchange: Determination of Interdiffusion Coefficients," *Ind. Eng. Chem. Fund.*, **23**, 400 (1984).

Glaski, F. A., and J. S. Dranoff, "Ion Exchange Kinetics: A Comparison of Models," *AIChE J.*, **9**(3), 427 (1963).

Gopala Rao, M., and M. M. David, "Single-Particle Studies of Ion Exchange in Packed Beds: Cupric Ion-Sodium Ion System," *AIChE J.*, **10**(2), 213 (1964).

Graham, E. E., "Application of Stefan-Maxwell Equation to Multicomponent Ion Exchange," *Fundamentals and Applications of Ion Exchange*, L. Liberty and J. R. Miller, eds., NATO, ASI Series, Martinus Nijhoff Publishers, The Netherlands (1985).

Graham, E. E., and J. S. Dranoff, "Application of Stefan-Maxwell Equations to Diffusion in Ion Exchangers: 1. Theory," *Ind. Eng. Chem. Fund.*, **21**, 360 (1982).

Graham, E. E., and J. S. Dranoff, "Application of Stefan-Maxwell Equations to Diffusion in Ion Exchangers: 2. Experimental Results," *Ind. Eng. Chem. Fund.*, **21**, 365 (1982).

Helfferich, F., "Ion Exchange Kinetics," in *Ion Exchange*, Chap. 2, J. A. Marinsky, ed., Marcel Dekker, New York (1966).

Helfferich, F., "Ion Exchange Kinetics. Vs. Ion Exchange Accompanied by Chemical Reactions," *J. Phys. Chem.*, **69**(4), 1178 (1965).

Helfferich, F., *Ion Exchange*, McGraw-Hill, New York (1962a).

Helfferich, F., "Ion Exchange Kinetics: III. Experimental Test of the Theory of Particle Diffusion Controlled Ion Exchange," *J. Phys. Chem.*, **66**(1), 39 (1962b).

Helfferich, F., and M. S. Plesset, "Ion Exchange Kinetics: A Nonlinear Diffusion Problem," *J. Chem. Phys.*, **28**(3), 418 (1958a).

Hering, B., and H. Bliss, "Diffusion in Ion Exchange Resins," *AIChE J.*, **9**(4), 495 (1963).

Kataoka, T., H. Yoshida, and H. Sanda, "Estimation of the Resin Phase Diffusivity in Isotopic Ion Exchange," *J. Chem. Eng. Japan*, **7**(2), 105 (1974).

Kraaijeveld, G., and J. A. Wesselingh, "The Kinetics of Film Diffusion-Limited Ion Exchange," *Chem. Eng. Sci.*, **48**(3), 467 (1993).

Krishna, R., "Diffusion in Multicomponent Electrolyte Systems," *Chem. Eng. J.*, **35**, 19 (1987).

Kuo, J. C. W., and M. M. David, "Single Particle Studies of Cation

Exchange Rates in Packed Beds: Barium Ion-Sodium Ion Systems," *AIChE J.*, **9**(3), 365 (1963).
Liberti, L., and R. Passino, "Ion Exchange Kinetics in Selective Systems," *Ion Exchange and Solvent Extraction*, Chap. 3, J. A. Marinsky and Y. Marcus, eds., Marcel Dekker, New York (1985).
Miller, J. R., D. G. Smith, W. E. Marr, and T. R. E. Kressmann, "Solvent-Modified Polymer Networks: I. The Preparation and Characterization of Expanded Network and Macroporous Styrene Divinyl Benzene Copolymers and Their Sulphonates," *J. Chem. Soc.*, 218 (1963).
Morig, C. R., and M. Gopala Rao, "Diffusion in Ion Exchange Resins: Sodium Ion-Strontium Ion System," *Chem. Eng. Sci.*, **20**, 889 (1965).
Morrison, Jr., F. A., and J. F. Osterle, "Electrokinetic Energy Conversion in Ultrafine Capillaries," *J. Chem. Phys.*, **43**(6), 2111 (1965).
Neale, G. H., and W. K. Nader, "Porous Media: Diffusive Flow Processes within an Homogeneous Swarm of Spherical Particles," *AIChE J.*, **19**(1), 112 (1973).
Pinto, N. G., and E. E. Graham, "Characterization of Resin Phase Diffusivities in Ion Exchange Resins," *Ind. Eng. Chem. Fundam.*, **26**, 2331 (1987).
Plesset, M. S., F. Helfferich, and J. N. Franklin, "Ion Exchange Kinetics: A Nonlinear Diffusion Problem: II. Particle Diffusion Control Exchange of Univalent and Bivalent Ions," *J. Chem. Phys.*, **29**(5), 1064 (1958b).
Reichenberg, D., "Properties of Ion-Exchange Resins in Relation to Their Structure. III Kinetics of Exchange," *J. Amer. Chem. Soc.*, **75**, 589 (1953).
Robinson, R. A., and R. M. Stokes, *Electrolyte Solutions*, Butterworths Scientific Publications, London (1959).
Schlögl, R., and F. Helfferich, "Comment on the Significance of Diffusion Potentials in Ion Exchange Kinetics," *J. Chem. Phys.*, **26**, 5 (1957).
Smith, T. G., and J. S. Dranoff, "Film Diffusion-Controlled Kinetics in Binary Ion Exchange," *Ind. Eng. Chem. Fund.*, **3**(3), 195 (1964).
Tetenbaum, M., and H. P. Gregor, "Self-Diffusion of Cations, Non-Exchange Anions, and Solvent in a Cation Exchange Resin System," *J. Phys. Chem.*, **58**, 1156 (1954).
Turner, J. C. R., "Nernst-Planck or No," *Fundamentals and Applications of Ion Exchange*, L. Liberty and J. R. Miller, eds., NATO, ASI series, Martinus Nijhoff Publishers, The Netherlands (1985).
Turner, J. C. R., and C. B. Snowdon, "Liquid-Side Mass-Transfer Coefficients in Ion Exchange: An Examination of the Nernst-Planck Model," *Chem. Eng. Sci.*, **23**, 321 (1968).
Turner, J. C. R., M. R. Church, A. S. W. Johnson, and C. B. Snowdon, "An Experimental Verification of the Nerst-Planck Model for Diffusion in an Ion Exchange Resin," *Chem. Eng. Sci.*, **21**, 317 (1966).
Vermeulen, T., M. D. LeVan, N. K. Hiester, and G. Klein, "Adsorption and Ion Exchange," in *Perry's Chemical Engineering Handbook*, 6th ed., R. H. Perry, D. W. Green, and J. O. Maloney, eds., p. 16-1.
Villadsen, J., and M. L. Michaelsen, *Solution of Differential Equation Models by Polynomial Approximation*, Prentice-Hall, Englewood Cliffs, NJ (1978).
Weatherley, L. R., and J. C. R. Turner, "Ion Exchange Kinetics—Comparison between a Macroporous and a Gel Resin," *Trans. Inst. Chem. Eng.*, **54**, 89 (1976).
Yoshida, H., and T. Kataoka, "Intraparticle Mass Transfer in Bidispersed Porous Ion Exchangers Part II. Mutual Ion Exchange," *Can. J. Chem. Eng.*, **63**, 430 (1985).

*Manuscript received July 5, 1994, and revision received Feb. 13, 1995.*